# An aerodynamic model for flapping-wing flight

**J. D. DeLaurier**
Institute of Aerospace Studies,
University of Toronto,
Downsview, Ontario, Canada

## ABSTRACT

A design-oriented model for the unsteady aerodynamics of a flapping wing has been developed using a modified strip theory approach. Within this constraint, vortex-wake effects are accounted for as well as partial leading edge suction and post stall behaviour. Also, the contributions of sectional mean angle of attack, camber, and friction drag are added, which allows this model to be used for the calculation of the average lift, as well as the thrust, power required, and propulsive efficiency of a flapping wing in equilibrium flight. An example of such calculations is presented in the performance prediction of a mechanical flying pterosaur replica.

## NOMENCLATURE

| | |
|---|---|
| $AR$ | Wing aspect ratio |
| $b/2$ | Semispan length |
| $c$ | Aerofoil chord |
| $h$ | Plunging displacement of leading edge in flapping direction |
| $C(k)_{Jones}$ | Finite-wing Theodorsen function |
| $C'(k)$ | Theodorsen function defined by Equation (8) |
| $C_d$ | Drag coefficient |
| $C_n$ | Normal force coefficient |
| $D$ | Drag |
| $F_x$ | Net chordwise force defined by Equation (21) |
| $F'(k)$, $G'(k)$ | Complex components of C'(k), given by Equation (9) |
| $k$ | Reduced frequency defined by Equation (7) |
| $L$ | Lift |
| $M$ | Pitching moment |
| $N$ | Force normal to the wing's chord |
| $P$ | Power |
| Rn | Reynolds number |
| $T$ | Thrust |
| $T_s$ | Leading edge suction force |
| $U$ | Flight speed |
| $V$ | Relative flow velocity at 1/4-chord location, given by Equation (13) |
| $w_o$ | Downwash velocity at the 3/4-chord location |
| $y$ | Coordinate along the semispan |
| $\alpha$ | Relative angle of attack at the 3/4-chord location due to the wing's motion |
| $\alpha'$ | The flow's relative angle of attack at the 3/4-chord location, given by Equation (4) |
| $\alpha_o$ | Angle of section's zero-lift line |
| $\beta_o$ | Magnitude of the dynamic twist's linear variation |
| $\delta\theta$ | Dynamically-varying pitch angle, $(\theta - \bar{\theta})$ |
| $\phi$ | Cycle angle, defined by Equation (33) |
| $\eta$ | Propulsive efficiency |
| $\eta_s$ | Leading edge suction efficiency |
| $\theta$ | Pitch angle of chord with respect to $U$ |
| $\bar{\theta}_a$ | Pitch angle of flapping axis with respect to $U$ |
| $\bar{\theta}_w$ | Mean pitch angle of chord with respect to flapping axis |
| $\rho$ | Atmospheric density |
| $\omega$ | Flapping frequency, rad/s |

### Subscripts

| | |
|---|---|
| $a$ | Apparent mass |
| $ac$ | Aerodynamic centre |
| $c$ | Circulation |
| $cf$ | Crossflow |
| $f$ | Friction |
| $in$ | Input |
| $out$ | Output |
| $sep$ | Separated flow |

### Superscripts

| | |
|---|---|
| – | Mean value |
| · | Time derivative |

Manuscript received 7 October 1991, accepted 22 January 1993.
Paper No. 1853.

## INTRODUCTION

The motivation for this work is based on an interest in mechanical flapping-wing flight. For that reason the analysis is very design oriented, capable of being readily implemented for the performance prediction of a variety of candidate configurations.

Most previous work seems to fall, roughly, into two categories. The first, and most common, is the quasi-steady model where unsteady wake effects are ignored. That is, flapping frequencies are assumed to be slow enough that shed wake effects are negligible. Although such an assumption gives a great simplification to the aerodynamic modelling, this category can still contain a wide range of sophistication in its detailed approaches. One of the simplest examples is given by Küchemann and von Holst[1] where a rigid elliptical-planform wing is assumed to be performing spanwise uniform motions, whereas Schmeidler[2, 3] presents a much

more detailed analysis using lifting-line theory to predict the performance of a root-flapping wing. One of the most refined versions of the lifting-line approach is offered by Betteridge and Archer[4], where they use their analysis to investigate the possibility of optimised flapping behaviour.

The quasi-steady approach also includes models of intermediate complexity, where the aerodynamic effects are concentrated at certain representative spanwise points on the wing. Walker[5] chooses three points along the semispan of a root-flapping wing, and assumes the motion to be such that the lift and drag are constant values on the downstroke and different constants on the upstroke. Norberg[6] chooses a single representative point, at 70% of the semispan, performing sinusoidal motion with constant lift-curve slope coefficients throughout the flapping cycle.

The second category accounts for the unsteady aerodynamic effects by modelling the wake in a variety of ways. Among those analyses that include the mean lift required for equilibrium flight (as compared with studies of animal swimming), Philps, East, and Pratt[7] represent the unsteady wake of a root-flapping non twisting rigid wing with discrete nonplanar vortex elements which include spanwise vortices spaced one per half cycle aft of the quarter-chord bound vortex. A similar model was developed by Blackwell and Archer[8] for their study of the propulsive characteristics of a twisting wing, root flapping with constant, but unequal, upstroke and downstroke motions ("sawtooth motion").

All of the above analyses assume that the wing is spanwise rigid. That is, the wing's semispan length (measured along a spanwise axis moving with the wing) is assumed to stay constant throughout the flapping motion's full cycle. A remarkable departure from this time-honoured assumption was offered by Rayner[9] when, upon noting that a lifting wing can produce negative thrust on the upstroke, he formulated a model assuming the wing to be aerodynamically active only on the downstroke. Thus, the vortex wake is a series of closed rings. However, Lighthill[10] noted how the lift requirement for most bird flight compels some aerodynamic activity on the upstroke, and described an extension of Rayner's model[11] in which upstroke lift is allowed, but that a span difference between upstroke and downstroke produces the net thrust.

The present analysis does not assume a variable span. Since the motivation was to study the feasibility of mechanical flapping-wing flight, it was felt that an important first step was to see if this was achievable without having to envision a span variation mechanism. However, the kinematics do allow for spanwise bending and twisting.

Further, this model assumes a continuous sinusoidal motion, with equal times between the upstroke and downstroke. This, along with the high aspect ratio envisioned for the wing, justified the assumption of a modified strip theory where the finite span unsteady-wake effects are accounted for by modified Theodorsen functions.

This analysis also differs from previous work in that camber and partial leading edge suction effects are accounted for. Too often, researchers interested in animal flight have chosen, as their starting point, an inviscid flow theory which assumes 100% leading edge suction. However, the reality is that the wings of flying animals can be highly cambered with little, if any, leading edge suction.

Post stall behaviour is accounted for in this analysis. It may well be that the variable span model for flapping flight can realistically allow totally attached flow. However, flapping wings with the presently assumed kinematics appear to be characterised by significant flow separation over portions of the cycle. In fact, such behaviour may not be undesirable for producing the average lift and thrust required for sustained flight. An example is shown of an efficiently designed model pterosaur wing for which this theory predicted, and experiment showed, significant outer panel flow separation.

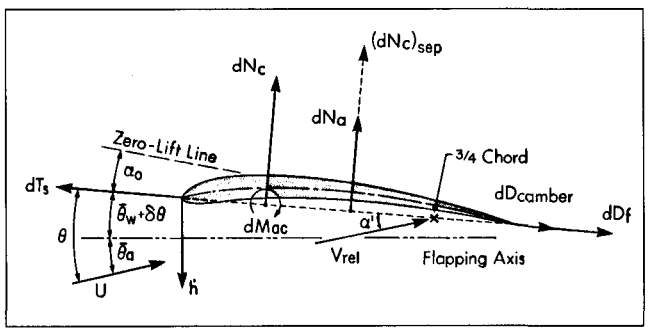


Figure 1. Wing section aerodynamic forces and motion variables.

## METHOD OF ANALYSIS

The kinematics for each section of the wing are illustrated in Figure 1. Upon using the leading edge as a reference point, the section's motion consists of a plunging velocity, $\dot{h}$, and a pitch angle, $\theta$. Note that $\dot{h}$ is not necessarily perpendicular to the mean-stream velocity, $U$. If the wing is root flapping, as shown in Fig. 2, then $\dot{h}$ would be perpendicular to the flapping axis.

The wing's aspect ratio is assumed to be large enough that the flow over each section is essentially chordwise (in the mean-stream direction). Therefore, the section's circulatory normal force is given by

$$dN_c = \frac{\rho U V}{2} C_n(y) c\,dy \qquad \ldots (1)$$

$V$ is the flow's relative velocity at the 1/4-chord location, and

$$C_n(y) = 2\pi\left(\alpha' + \alpha_0 + \bar{\theta}\right) \qquad \ldots (2)$$

The parameters in Equation (2) are illustrated in Fig. 1, where it is seen that the angle of the zero lift line, $\alpha_o$, is a fixed value for the aerofoil, and $\bar{\theta}$ is the section's mean pitch angle. Further, $\bar{\theta}$ is given by the sum:

$$\bar{\theta} = \bar{\theta}_a + \bar{\theta}_w \qquad \ldots (3)$$

where $\bar{\theta}_a$ is the angle of the flapping axis with respect to the mean-stream velocity, $U$, and $\bar{\theta}_w$ is the mean angle of the chord with respect to the flapping axis. Note that if the wing does not have a flapping axis (such as for whole-wing motions), then $\bar{\theta}$ is the wing's mean pitch angle.

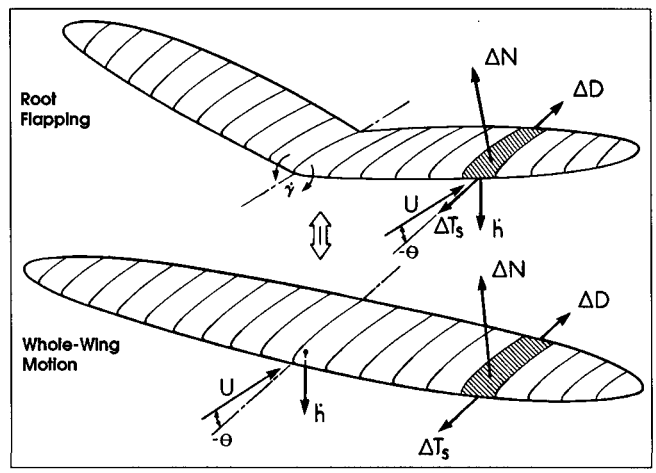


Figure 2. Assumed strip theory equivalence to whole wing motion.

The remaining angle in Equation (2), $\alpha'$, is given by

$$\alpha' = \left[\frac{ARC'(k)}{(2+AR)}\right]\alpha - \frac{w_0}{U} \qquad \ldots (4)$$

where $\alpha$ is the relative angle of attack at the 3/4-chord location due to the wing's motion:

$$\alpha = \frac{\left(\dot{h}\mathrm{Cos}\left(\theta - \bar{\theta}_a\right) + \frac{3}{4}c\dot{\theta} + U\left(\theta - \bar{\theta}\right)\right)}{U} \qquad \ldots (5)$$

The coefficient of $\alpha$ in Equation (4) accounts for the wing's finite-span unsteady vortex wake by means of a strip theory model. As illustrated in Fig. 2, each chordwise strip on the wing is assumed to act as if it were part of an elliptical planform wing, of the same aspect ratio, executing simple harmonic whole wing motions identical to that of the strip's. For such a wing, Jones[12] derived that the unsteady normal-force coefficient, $\delta C_n$, is given by

$$\delta C_n = 2\pi C(k)_{Jones}\alpha \qquad \ldots (6)$$

Where $C(k)_{Jones}$ is a modified Theodorsen function for finite $AR$ wings and $k$ is the reduced frequency, given by

$$k = \frac{c\omega}{2U} \qquad \ldots (7)$$

$C(k)_{Jones}$ is a complex function, and it was found convenient to use Scherer's[13] alternative formulation:

$$C(k)_{Jones} = \frac{ARC'(k)}{(2+AR)} \qquad \ldots (8)$$

where, for the complex terms given by

$$C'(k) = F'(k) + iG'(k) \qquad \ldots (9)$$

Scherer presents the approximate equations:

$$F'(k) = 1 - \frac{C_1 k^2}{\left(k^2 + C_2^2\right)}$$

$$G'(k) = -\frac{C_1 C_2 k}{\left(k^2 + C_2^2\right)}$$

$$C_1 = \frac{0{\cdot}5AR}{(2{\cdot}32 + AR)}$$

$$C_2 = 0{\cdot}181 + \frac{0{\cdot}772}{AR}$$

Upon noting that the assumed motion is given by

$$\alpha = Ae^{i\omega t} \qquad \ldots (10)$$

one obtains, when Equations (7), (9), and (10) are substituted into Equation (4), that

$$\alpha' = \frac{AR}{(2+AR)}\left[F'(k)\alpha + \frac{c}{2U}\frac{G'(k)}{k}\dot{\alpha}\right] - \frac{w_0}{U} \qquad \ldots (11)$$

The downwash term, $w_o/U$, is due to the mean lift produced by $\alpha_o$ and $\bar{\theta}$, and it may be calculated in a variety of ways. If one wished to stay consistent with the strip theory model assumed for the unsteady aerodynamic terms, then $w_o/U$ could be approximated by the downwash for an untwisted elliptical-planform wing, obtained from Kuethe and Chow[14]:

$$\frac{w_0}{U} = \frac{2\left(\alpha_0 + \bar{\theta}\right)}{2+AR} \qquad \ldots (12)$$

However, if the wing has significant spanwise variation of $\alpha_o + \bar{\theta}$, then one may wish to calculate $w_o/U$ by a more accurate method, such as the extended lifting-line theory for twisted wings described in Ref. 14.

Returning to Equation (1), note that the flow velocity, $V$, must include the downwash as well as the wing's motion relative to $U$. This is accomplished by including $\alpha'$ along with the kinematic parameters:

$$V = \left\{\left[U\mathrm{Cos}\theta - \dot{h}\mathrm{Sin}\left(\theta - \bar{\theta}_a\right)\right]^2 + \left[U\left(\alpha' + \bar{\theta}\right) - \frac{1}{2}c\dot{\theta}\right]^2\right\}^{\frac{1}{2}} \qquad \ldots (13)$$

An additional normal force contribution comes from the apparent mass effect, which acts at the midchord (see Fig. 1) and is given by

$$dN_a = \frac{\rho\pi c^2}{4}\dot{v}_2 dy \qquad \ldots (14)$$

where $\dot{v}_2$ is the time rate of change of the midchord normal velocity component due to the wing's motion:

$$\dot{v}_2 = U\dot{\alpha} - \frac{1}{4}c\ddot{\theta} \qquad \ldots (15)$$

Therefore, the section's total attached flow normal force is

$$dN = dN_c + dN_a \qquad \ldots (16)$$

The section's circulation distribution likewise generates forces in the chordwise direction, as illustrated in Fig. 1. From DeLaurier[15], the chordwise force due to camber is given by

$$dD_{camber} = -2\pi\alpha_0\left(\alpha' + \bar{\theta}\right)\frac{\rho UV}{2}cdy \qquad \ldots (17)$$

Garrick's[16] expression for the leading edge suction of a two dimensional aerofoil may be applied to the present strip theory model by extending it with Equation (4) to obtain

$$dT_s = \eta_s 2\pi\left(\alpha' + \bar{\theta} - \frac{1}{4}\frac{c\dot{\theta}}{U}\right)^2\frac{\rho UV}{2}cdy \qquad \ldots (18)$$

The efficiency term, $\eta_s$, accounts for the fact that most aerofoils, due to viscous effects, have less than the 100% leading edge suction predicted by potential-flow theory.

Viscosity also gives a chordwise friction drag

$$dD_f = \left(C_d\right)_f\frac{\rho V_x^2}{2}cdy \qquad \ldots (19)$$

where $V_x$ is the flow speed tangential to the section, approximated by

$$V_x = U\mathrm{Cos}\theta - \dot{h}\mathrm{Sin}\left(\theta - \bar{\theta}_a\right) \qquad \ldots (20)$$

and $(C_d)_f$ is the drag coefficient due to skin friction, for which expressions may be found in Hoerner[17]. Thus, the total chordwise force is

$$dF_x = dT_s - dD_{camber} - dD_f \qquad \ldots (21)$$

An advantage of the strip theory model is that it allows for an approximation to localised post stall behaviour. The dynamic stall angle is obtained from Prouty[18]

$$\alpha_{stall} = \left(\alpha_{stall}\right)_{static} + \xi\left[\frac{c\dot{\alpha}}{2U}\right]^{\frac{1}{2}} \qquad \ldots (22)$$

and is chosen to apply at the leading edge. Therefore, the criterion for attached flow over the section is

$$\left(\alpha_{stall}\right)_{min} \le \left[\alpha' + \bar{\theta} - \frac{3}{4}\left(\frac{c\dot{\theta}}{U}\right)\right] \le \left(\alpha_{stall}\right)_{max} \qquad \ldots (23)$$

When the attached flow range is exceeded, totally separated flow is assumed to abruptly occur, for which condition all chordwise forces are negligible:

$$dD_{camber}, dT_s, dD_f = 0 \quad \ldots (24)$$

and the normal force is given by

$$dN = (dN_c)_{sep} + (dN_a)_{sep} \quad \ldots (25)$$

$(dN_c)_{sep}$, shown in Fig. 1, is due to crossflow drag:

$$(dN_c)_{sep} = (C_d)_{cf} \frac{\rho \hat{V} V_n}{2} c\,dy \quad \ldots (26)$$

where

$$\hat{V} = \left(V_x^2 + V_n^2\right)^{\frac{1}{2}} \quad \ldots (27)$$

and $V_n$ is the midchord normal velocity component due to the wing's motion (note that $\dot{v}_2$, in Equation (15), is the linearised time-derivative of $V_n$):

$$V_n = \dot{h}\mathrm{Cos}\left(\theta - \bar{\theta}_a\right) + \frac{1}{2}c\dot{\theta} + U\mathrm{Sin}\theta \quad \ldots (28)$$

Also, $(dN_a)_{sep}$ is due to apparent-mass effects, assumed to be half that of the attached flow value in Equation (14):

$$(dN_a)_{sep} = \frac{1}{2} dN_a \quad \ldots (29)$$

Now, the equations for the segment's instantaneous lift and thrust are

$$dL = dN\mathrm{Cos}\theta + dF_x \mathrm{Sin}\theta \quad \ldots (30)$$

$$dT = dF_x \mathrm{Cos}\theta - dN\mathrm{Sin}\theta \quad \ldots (31)$$

These may be integrated along the span to give the whole wing's instantaneous lift and thrust:

$$L(t) = 2\int_0^{\frac{b}{2}} \mathrm{Cos}\gamma\, dL$$
$$T(t) = 2\int_0^{\frac{b}{2}} dT \quad \ldots (32)$$

where $\gamma(t)$ is the section's dihedral angle at that instant in the flapping cycle.

The wing's average lift and thrust are obtained by integrating $L(t)$ and $T(t)$ over the cycle. To do this, it was found most convenient to perform the integration with respect to cycle angle, $\phi$, instead of time, $t$, where

$$\phi = \omega t \quad \ldots (33)$$

so that the average lift and thrust are expressed as

$$\bar{L} = \frac{1}{2\pi}\int_0^{2\pi} L(\phi)d\phi$$
$$\bar{T} = \frac{1}{2\pi}\int_0^{2\pi} T(\phi)d\phi \quad \ldots (34)$$

One may also obtain the instantaneous power required to move the section against its aerodynamic loads. For attached flow, this is given by

$$dP_{in} = dF_x \dot{h}\mathrm{Sin}\left(\theta - \bar{\theta}_a\right) + dN\left[\dot{h}\mathrm{Cos}\left(\theta - \bar{\theta}_a\right) + \frac{1}{4}c\dot{\theta}\right]$$
$$+ dN_a\left[\frac{1}{4}c\dot{\theta}\right] - dM_{ac}\dot{\theta} - dM_a\dot{\theta} \quad \ldots (35)$$

where $dM_{ac}$ is the section's pitching moment about its aerodynamic centre, and $dM_a$ includes apparent-camber and apparent-inertia moments:

$$dM_a = -\left[\frac{1}{16}\rho\pi c^3\dot{\theta}U + \frac{1}{128}\rho\pi c^4\ddot{\theta}\right]dy \quad \ldots (36)$$

For separated flow, the input power expression becomes

$$dP_{in} = dN_{sep}\left[\dot{h}\mathrm{Cos}\left(\theta - \bar{\theta}_a\right) + \frac{1}{2}c\dot{\theta}\right] \quad \ldots (37)$$

The instantaneous aerodynamic power absorbed by the whole wing is found from

$$P_{in}(t) = 2\int_0^{\frac{b}{2}} dP_{in} \quad \ldots (38)$$

and the average input power, throughout the cycle, is given by

$$\bar{P}_{in} = \frac{1}{2\pi}\int_0^{2\pi} P_{in}(\phi)d\phi \quad \ldots (39)$$

Upon noting that the average output power from the wing is

$$\bar{P}_{out} = \bar{T}U \quad \ldots (40)$$

the average propulsive efficiency may be calculated from

$$\bar{\eta} = \frac{\bar{P}_{out}}{\bar{P}_{in}} \quad \ldots (41)$$

## NUMERICAL EXAMPLE

In the mid 1980s, the National Air and Space Museum in Washington DC contracted the AeroVironment Corporation of Monrovia California to design and construct a giant flying robot pterosaur[19]. This challenging task produced remarkable research in several areas, including computerised stability augmentation and flight control systems, as well as providing an engineering reinterpretation of paleontological evidence.

The author was requested by AeroVironment to apply the flapping-wing analysis described above to a performance prediction of the completed 18 ft-span model. The 40 lb total weight (mainly due to onboard batteries) plus the drag of the fur-like covering, was evidently preventing sustained flapping flight. Although AeroVironment had done its own aerodynamic predictions, an independent check was desired. The author and his associate, Jeremy Harris of Battelle Memorial Institute, were pleased to perform these calculations for this unusual aircraft.

The wing's planform geometry is illustrated in Fig. 3, where the inflight static twist distribution, $\bar{\theta}_w$, is designed to be zero. The aerofoil along the span is the Liebeck LPT 110A , for which it was calculated that

$$\alpha_0 = 0{\cdot}5^\circ$$
$$\eta_s = 0{\cdot}98$$
$$C_{mac} = 0{\cdot}025 \quad \ldots (42)$$
$$(\alpha_{stall})_{max} = 13^\circ$$

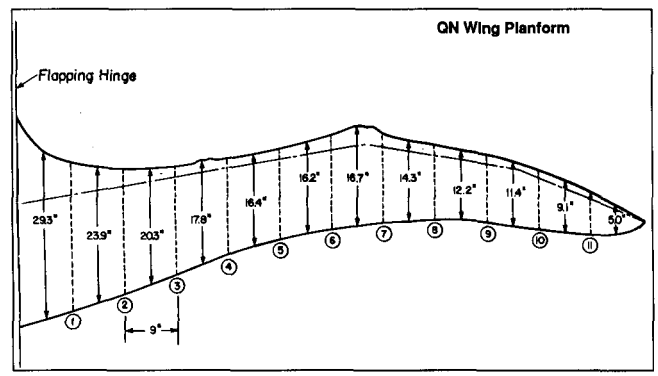


Figure 3. Wing planform of the QN pterosaur model.

It was assumed, for this example, that negative-$\alpha'$ stalling would not occur. Therefore, $(\alpha_{stall})_{min}$ was not specified. Also, at the time this work was performed, the dynamic-stall criterion had not yet been incorporated into the analysis. Thus $\xi$, from Equation (22), was effectively zero.

The texture of the wing's surface is such as to produce a full chord turbulent boundary layer, so that the friction drag was obtained from Ref. 17 as:

$$(C_d)_f = \frac{0{\cdot}89}{[\log(\mathrm{Rn})]^{2{\cdot}58}} \quad \ldots (43)$$

where Rn is based on the local chord. Further, the post stall normal force coefficient, $(C_d)_{cf}$, was chosen to be that for a high-$AR$ flat plate, given by Ref. 20 as 1·98.

Root flapping kinematics are assumed, with no spanwise bending. Therefore, the plunging motion is given by

$$h = -(\Gamma y)\mathrm{Cos}\phi \quad \ldots (44)$$

where $\Gamma$ is the maximum flapping angle magnitude, given as 0·3491 rad (20°).

The dynamic twisting, $\delta\theta$, is likewise assumed to vary linearly along the span, so that

$$\delta\theta = -(\beta_0 y)\mathrm{Sin}\phi \quad \ldots (45)$$

For this study, $\beta_0$ was chosen as a variable. Further, note that the above equations fix the phasing between plunging and pitching at – 90°.

Discrete element integrations of Equations (32), (34), (38), and (39) were performed. For example, by assuming the time integration to be approximated by a summation at discrete cycle increments, $\phi_j$ ($j$ = 1 to $m$), Equation (34) becomes

$$\bar{L} \cong \frac{1}{m}\sum_{j=1}^{m} L_j \quad \ldots (46)$$

Also, from Equation (32), one may approximate $L_j$ by

$$L_j \cong 2\sum_{i=1}^{n} \mathrm{Cos}\gamma_{ij}\Delta L_{ij} \quad \ldots (47)$$

where $i$ refers to station locations along the wing's semispan, $y_i$, ($i$ = 1 to $n$). This means, for the equations presented in the previous Section, that $dy$ is replaced by a finite increment $\Delta y$, which is centred about $y_i$ with corresponding values for $c_i$, $\bar{\theta}_i$, etc. For the example, equal $\Delta y$ increments of 6 in were chosen, giving $n$ = 12. Also, $m$ = 20 was selected for the time intervals.

The results are shown in Figs 4 and 5 where, for the given flapping frequency of 1·2 Hz, it is seen that the wings will lift the model's 40 lb weight if the flapping-axis angle, $\bar{\theta}_a$, equals 7·5°, the flight speed, $U$, equals 44 ft/s, and the dynamic twist magnitudes, $\beta_o$, are in excess of 2·2°/ft. Beyond this, the lift stays fairly constant up to the highest $\beta_o$ value considered (3·0°/ft).

The average thrust, however, achieves its maximum value of 1.2 lb within a very narrow range of $\beta_o$, namely ≈ 2·25°/ft. Beyond this, the thrust falls off rapidly to zero at $\beta_o \approx 2{\cdot}8$°/ft. This is also seen in the propulsive efficiency curve, where a distinct maximum of 42% is reached at the $\beta_o \approx 2{\cdot}25$°/ft value.

It should be mentioned that the flapping wing propulsive efficiency, as defined in this article, is not directly comparable to propeller efficiencies unless, for a given flight situation, the wing's drag were subtracted from the propeller's thrust. Therefore, the example flapping wing is a more efficient thruster than the 42% figure would indicate.

The average input power, $\bar{P}_{in}$, decreases steadily with $\beta_o$, which is simply an indication of how the wing requires less work to flap as the dynamic-twisting magnitudes increase. In fact, if $\beta_o$ increased much beyond 3·0°/ft, $\bar{P}_{in}$ would become negative,

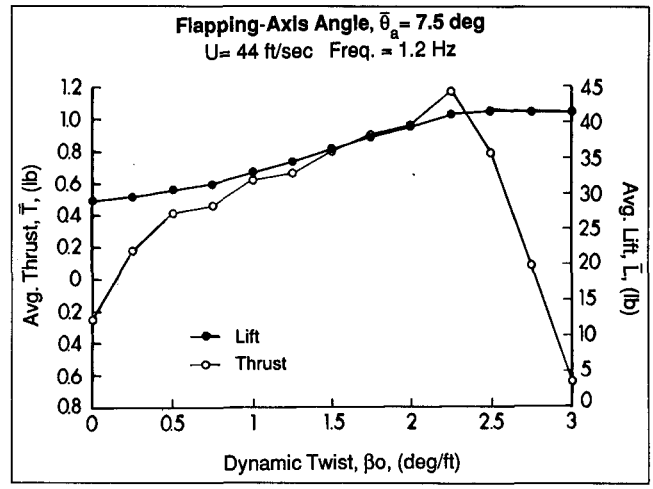


Figure 4. QN average lift and thrust performance.

indicating a "windmilling" situation where energy is taken from the 44 ft/s flow. It is seen that this occurs quite abruptly beyond the optimum $\beta_o$ condition.

It should be noted that, for engine sizing purposes, it is the peak value of input power that is required, not the average. For this example, the peak input power required to overcome the aerodynamic reaction forces and moments was calculated to be 800 watts.

For the $\beta_o \approx 2{\cdot}25$°/ft maximum efficiency case, the analysis predicted considerable stalling on the outboard panels during the downstroke. This was due, in large measure, to the high value of $\bar{\theta}_a$ required for equilibrium flight. Such behaviour was also observed during flow visualisation experiments by AeroVironment.

Finally, although the optimum $\beta_o \approx 2{\cdot}25$°/ft dynamic twist distribution appeared to identify a condition for sustained flight, tests of the QN aircraft showed only powered glides. One reason may be that the optimum $\beta_o$ requirement allows virtually no error, which would be difficult to implement in practice. Additionally, there may have been significant differences between the actual and predicted behaviour of the aerofoil. For example, flight tests showed that the fur-like covering evidently gave more drag than a smooth skin. This would require expression by an increase in the $(C_D)_f$ values used in this analysis, thus reducing thrusting ability. Also, when the author inspected the aircraft at the National Air and Space Museum, it appeared that the irregularity of the covering around the leading edge would significantly decrease the leading edge suction efficiency from its predicted value of $\eta_s$ = 0·98. It

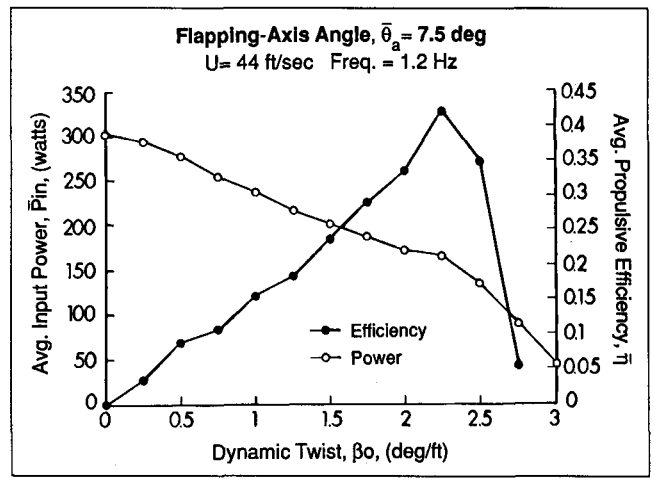


Figure 5.QN average input power and propulsive efficiency.

is difficult to see how this could have been avoided, considering the constraints imposed by the requirements for realism in appearance and kinematics. However, a reduction in $\eta_s$ likewise reduces the wing's thrusting ability. Considering that the margin for sustained flight was fairly narrow to begin with, any of the above reasons could have sufficiently compromised the aircraft's performance.

## CONCLUSIONS

This article has presented a design-oriented method by which one may predict the flight performance of harmonically flapping wings. The major assumptions are that, first, the semispan remains constant throughout the motion; and second, a modified strip theory is used to model the aerodynamics. However, general distributions of spanwise twisting and first order bending may be specified. Also, certain important real fluid effects are accounted for, such as post stall behaviour and partial leading edge suction. These are features which should be included in any accurate flapping-wing analyses, especially when applied to flying animals which usually have sharp edged wings with little leading edge suction.

When the analysis was applied to the Project QN mechanical pterosaur, it was found that sustained flight was only possible for a virtually singular dynamic twist distribution. The difficulty of mechanically implementing this, along with other considerations such as the aerofoil's "as built" *vs* theoretical performance, appeared to confirm the aircraft's inability to climb or sustain. It should be noted, though, that without the drag of the fur-like covering and the weight of the batteries for electric propulsion, the analysis indicates that such a flapping wing aircraft could readily achieve sustained flight. That is, the required lift and thrust may be obtained from a harmonically flapping constant semispan wing with localised flow separation.

This should be compared with the attached flow variable span model discussed in the Introduction, which appears to be an accurate representation for a spectrum of animal flight, especially at low speeds. The present analysis, however, shows that the constant-semispan model is also capable of efficient flapping-wing flight for certain conditions, such as may be experienced by large animals at high speeds, or ornithopter aircraft.

In fact, for the purposes of achieving mechanical flapping-wing flight, constant semispan motion has been the traditional approach by experimenters. Even if the designers had been aware of any variable span concept, the difficulty of its mechanical implementation (in addition to all the other challenges of ornithopter design) may well have discouraged its use. What is seen, however, is that a constant semispan wing holds the promise, if properly designed and incorporated, of producing the thrust and lift required for successful flapping-wing flight.

## ACKNOWLEDGEMENTS

This work was supported by an Operating Grant from the Natural Sciences and Engineering Research Council of Canada. The author appreciates the co-operation of the AeroVironment Corporation in making information on the QN Project available for this publication. Further, this work benefited greatly from the careful study and helpful suggestions of J.M. Harris, Principal Research Engineer at Battelle Memorial Institute, who also produced Figs 4 and 5.

## REFERENCES

1. KÜCHEMANN, D. and VON HOLST, E. Aerodynamics of animal flight, *Luftwissen*, September 1941, **8**, (9), pp 277-282, Translated by L.J. Baker for the Ministry of Aircraft Production, R.T.P. Translation No. 1672.
2. SCHMEIDLER, W. Dynamik des Schwingenfluges, *Luftfahrtforschung*, 1935, (4), pp 128-133.
3. SCHMEIDLER, W. Flugzeuge mit Flugelantrieb, *Luftfahrtforschung*, 1936, (4), pp 111-117.
4. BETTERIDGE, D.S. and ARCHER, R.D. A study of the mechanics of flapping wings, *Aeronaut Q*, May 1974, pp 129-142.
5. WALKER, G. The flapping flight of birds, *J R Aeronaut Soc*, 1927, **31**, pp 590-594.
6. NORBERG, U.M. Evolution of vertebrate flight: an aerodynamic model for the transition from gliding to active flight, *Am Naturalist*, September 1985, **126**, (3), pp 303-327.
7. PHILPS, P.J., EAST, R.A. and PRATT, N.H. An unsteady lifting-line theory of flapping wings with application to the forward flight of birds, *J Fluid Mech*, 1981, **112**, pp 97-125.
8. BLACKWELL, J. and ARCHER, R.D. Performance Characteristics of Simple Flapping Motion With Application to the Cruising Flight of Birds, University of New South Wales Report, 1985/FMT/1, ISSN 0156 3068.
9. RAYNER, J.M. A vortex theory of animal flight. Part 2. The forward flight of birds, *J Fluid Mech*, 1979, **91**, (4), pp 731-763.
10 LIGHTHILL, Sir James, Some challenging new applications for basic mathematical methods in the mechanics of fluids that were originally pursued with aeronautical aims, *Aeronaut J*, February 1990, **94**, (932), pp 41-52.
11. RAYNER, J. Vertebrate flapping flight mechanics and aerodynamics, and the evolution of flight in bats, *Biona-report 5*, Gustav Fischer, Stuttgart, 1986, pp 27-74.
12. JONES, R.T. The Unsteady Lift of a Wing of Finite Aspect Ratio, NACA Report No. 681, 1940.
13. SCHERER, J.O. Experimental and theoretical investigation of large amplitude oscillating foil propulsion systems, Hydronautics, Laurel, Md, December 1968.
14. KUETHE, A.M. and CHOW, C-Y. The finite wing, *Foundations of Aerodynamics*, 4th ed, John Wiley, New York, 1986, pp145-164.
15. DELAURIER, J. Drag of wings with cambered aerofoils and partial leading-edge suction, *J Aircr*, October 1983, **20**, (10), pp 882-886.
16. GARRICK, I.E. Propulsion of a Flapping and Oscillating Aerofoil, NACA Report No 567, 1936.
17. HOERNER, S.F. Skin-friction drag, *Fluid-Dynamic Drag*, Published by the Author, Brick Town, NJ, 1965, pp 2-1 to 2-16.
18 PROUTY, R.W. Airfoils for rotor blades, Helicopter Performance, Stability, and Control, PWS Engineering, Boston, 1986, pp 397-409.
19 BROOKS, A.N., MACCREADY, P.B., LISSAMAN, P.B.S. and MORGAN, W.R. Development of a wing-flapping flying replica of the largest Pterosaur, AIAA Paper 85-1446, 1985.
20. HOERNER, S.F. Pressure drag, *Fluid-Dynamic Drag*, Published by the Author, Brick Town, NJ, 1965, pp 3-16.

*Editors note: Two further papers on flapping-wing flight by Professor DeLaurier are due for publication in* The Aeronautical Journal.